Investigation of the antimicrobial properties of modified multilayer diamond-like carbon coatings on 316 stainless steel surface and coatings technology

Robertson, Shaun; Gibson, Desmond; MacKay, William; Reid, Stuart; Williams, Craig; Birney, Ross

Published in:
Surface & Coatings Technology

DOI:
10.1016/j.surfcoat.2016.11.035

Published: 25/03/2017

Document Version
Peer reviewed version

Investigation of the Antimicrobial Properties of Modified Multilayer Diamond-like Carbon Coatings on 316 Stainless Steel

Shaun N Robertson[a,b], Des Gibson[b], William G MacKay[a], Stuart Reid[b], Craig Williams[a] & Ross Birney[b]

[a]Institute of Healthcare, Policy and Practice, School of Health, Nursing and Midwifery, University of the West of Scotland, PA1 2BE Paisley, Scotland, UK

[b]SUPA, Institute of Thin Films, Sensors and Imaging, School of Engineering and Computing, University of the West of Scotland, PA1 2BE Paisley, Scotland, UK

AUTHOR INFORMATION

Shaun.Robertson@uws.ac.uk

Des.Gibson@uws.ac.uk

W.mackay@uws.ac.uk

Stuart.Reid@uws.ac.uk

Craig.Williams@uws.ac.uk

Corresponding Author

Ross.Birney@uws.ac.uk

Telephone number: +44(0)141 8494031

ABSTRACT:

Modified diamond-like carbon (DLC) coatings were deposited onto 25 mm diameter 316 stainless steel discs by pulsed (direct current) hollow cathode plasma enhanced chemical vapour deposition (HC-PECVD). Multilayer films of total thickness 1 – 2 µm were deposited, both with and without germanium dopant. Characterisation of the coatings was performed by SEM/EDX, surface energy/contact angle analysis, and assessment of possible biofilm-inhibiting properties. Both modified DLC and germanium-doped DLC (Ge-DLC) coatings showed a significant anti-biofouling effect on *P. aeruginosa,* a Gram-negative bacterium. A 90% reduction in *P. aeruginosa* biomass was observed compared to control for both DLC and Ge-DLC, however this effect could not be attributed to germanium incorporation alone. Neither modified DLC nor Ge-DLC showed a significant inhibitory effect on *S. aureus,* a Gram-positive bacterium. Scanning electron microscopy of *P. aeruginosa* biofilms on Ge-DLC coated 316 stainless steel clearly displayed disruption of the cellular wall, as well as leakage of cellular components; this effect was not observed with modified DLC coating. This suggests that germanium-doped DLC coatings may potentially exhibit a cidal mode of action versus *P. aeruginosa* biofilms.

KEYWORDS: Modified diamond like carbon, microbial biofilm prevention, anti-biofouling

1. Introduction

Microbial biofilms are ubiquitous in aqueous environments, including but not limited to pipelines, food & beverage industry, ship hulls and heat exchangers; in fact, biofouling may occur on virtually any surface in contact with water [1, 2]. With biofilm formation on such surfaces there are significant implications. For example, internal diameter is reduced in pipes, leading to reduced flow rates; microbial influenced corrosion of metals [3], leading to damage and subsequently necessitating the replacement of pipelines; and increased drag of ships, leading to higher fuel consumption with the associated environmental impacts [4]. Notably, microbial biofilms have the potential to act as reservoirs of infection in potable and washing water systems, which can have a devastating impact on community [5, 6] and healthcare related environments [7].

A biofilm can briefly be described as a consortium of cells, encapsulated within an extracellular polymeric substance (EPS) [8, 9]. The EPS provides them with a high degree of hydration, and strong attachment to a surface when compared to the initial planktonic cell attachments preceding biofilm formation; and, in turn, increased resistance to removal via cleaning [10]. For example, chlorine may prove to be ineffective in treating established biofilms [11, 12].

Methods to prevent microbial attachment, through the development of antimicrobial coatings for industrial and clinical settings, are highly sought after in order to combat the increasing costs and morbidity/mortality that can be associated with biofilms. Diamond-like carbons (DLCs) have found utility in a wide range of applications, perhaps most notably as protective coatings for metals against corrosion [13-16]. DLCs represent a class of amorphous carbon materials; the main subtypes being amorphous hydrogen-carbon alloy (a-C:H), hydrogen-free amorphous carbons (a-C) and tetrahedrally-structured amorphous carbons and their hydrogenated analogues (ta-C and ta-C:H), which can contain in excess of 90% C-C sp^3 bonding. Previous research into silicon-doped DLC has shown reduction in

biofouling, with the common Gram-negative bacteria *Pseudomonas aeruginosa* and Gram-positive bacteria *S. aureus* and *S. epidermidis* [17, 18]. Doping of DLC with known antimicrobial metals such as copper [19], silver, and platinum [20], has been undertaken, but this often involves the incorporation of metallic nanoparticles in and on the upper layer of the DLC. Recent research has demonstrated that nanoparticles (NPs) have even greater cytotoxicity than non-nanoparticle forms of such metals [21-24], potentially precluding their use in healthcare and environmental applications, if a suitable concentration window cannot be achieved. Research has also shown that ion release from NPs incorporated into DLC coatings is dependent on nanoparticle size, with increasing ion release being related to decreasing NP size, which allows tailoring of the antibacterial and toxicity windows for medical implants [25]. An additional problem highlighted in prior literature on the anti-biofouling effects of doped DLC is the common use of colony-forming unit (CFU) tests to test the coatings' properties. These tests are often performed by dropping small quantities of an inoculum onto a surface, either in sterile water or phosphate buffered saline (PBS) solution. However, the planktonic minimum inhibitory concentrations (MIC) can differ markedly versus the minimum biofilm eradication concentration (MBEC). This is clearly evidenced in the clinical setting [26], with antimicrobial drugs often having MBECs that can be up to 100 times greater than the MIC; in some cases, they are completely ineffective. This observation is not limited to conventional antimicrobials, with concentrations of silver required to eradicate mature *P. aeruginosa* biofilms being 10-100 times greater than the MIC of planktonic cultures [27].

Germanium is a metalloid from the carbon group, and is chemically similar to silicon. Elemental germanium in suspension has been shown to have antimicrobial properties versus *P. aeruginosa* and *Staphylococcus aureus* in both planktonic (MIC = 6.25 mg/ml) and biofilm (MBEC 25 & 50 mg/ml respectively) [28]. In this work, a hollow cathode plasma enhanced chemical vapour deposition (HC-PECVD) system (Sub-One Systems, Tucson, AZ), specifically designed for coating interior pipe surfaces, was used to deposit multi-layer modified DLC coatings and germanium-doped multi-layer

DLC (Ge-DLC) coatings; the optimized DLC and Ge- DLC were then evaluated to assess for any biofilm-inhibiting and antimicrobial properties.

2. Materials and methods

2.1 Preparation of DLC and Ge-DLC

Multilayer modified DLC and Ge-DLC coatings were deposited onto 25 mm diameter 316 stainless steel discs by pulsed-DC hollow cathode plasma enhanced vapour deposition (HC-PECVD) deposition as previously described elsewhere [29, 30]. However, in this current work, an aluminium stage (Figure 1) was fabricated; designed to conform to the interior of a 4" pipe (cathode) and to accommodate planar substrates. This stage ensured that the substrates remained in electrical contact with the cathode; this was necessary to enable film deposition on the stainless steel discs. SS316 and silicon wafer witness substrates were initially cleaned with acetone and lint free cloth to ensure a contaminant-free surface and a base pressure of $1x10^{-3}$ Torr was attained in the chamber prior to deposition. A hydrogen and argon plasma substrate pre-heating step was performed, followed by an argon-only sputter etch, which has previously been shown to enhance adhesion of multilayer DLC [2, 31, 32].

Both the DLC and Ge-DLC coatings were 5-layer graded designs deposited with argon as the working gas, and using tetramethylsilane (TMS, $Si(CH_3)_4$), acetylene (C_2H_2) and, in the case of the Ge-doped coating, finally tetramethylgermane (TMGe, $Ge(CH_3)_4$) in the top layer. These coatings were deposited in a multi-stage process, beginning with TMS, which results in deposition of an amorphous SiC:H adhesion layer; with increasing fraction of acetylene and decreasing fraction of TMS in the following layer steps, terminating with either an a-C:H or Ge-doped a-C:H top layer.

The deposition processes are summarized in table 1.

Table 1. Summary of deposition processes

Step	Ar (sccm)	H_2 (sccm)	C_2H_2 (sccm)	TMS	TMGe	Pressure (mTorr)	Anode Power (W)	Cathode Power (W)	Time (min. :s)
1	50	100	-	-	-	70	35	180	0:30
2	50	100	-	-	-	70	40	200	10:00
3	100	-	-	-	-	70	40	200	30:00
4	100	-	-	-	-	70	40	200	0:20
5	90	-	-	70	-	120	40	144	0:54
6	60	-	20	60	-	70	40	216	0:54
7	50	-	40	40	-	70	52	136	0:54
8	50	-	80	20	-	70	52	136	0:54
9	50	-	120 (**108**)	-	0 **(12)**	90	52	136	1:30
10	85(+200 N_2)	-	-	-	-	Purge	-	-	2:00

Bold type indicates parameters during Ge-DLC coating deposition.

2.2 Characterisation of DLC and Ge-DLC coatings

2.2.1 SEM and EDX analysis

Characterisation of the multilayer modified DLC and Ge-DLC coatings was performed by scanning electron microscope (SEM) analysis of both the surface and cross-section of coated silicon wafer witness pieces. Analysis was performed on a Hitachi S-4100 scanning electron microscope at 10 kV acceleration voltage. Composition of the upper layers of the DLC thin film was determined by energy dispersive x-ray (EDX) analysis of the witness piece on an Oxford instruments X-Max 80 detector at three acceleration voltages (10, 15 & 20 kV); this allows elemental composition to be determined at varying depths within the multilayer sample.

2.2.2 Surface roughness characterisation

Average surface roughness measurements were performed on a Dektak 3ST surface profilometer (Veeco, USA). Surface roughness scans were performed in triplicate on each sample, with the following measurement parameters: scan length 2000 μm (1000 data points over scan length), 30 mg

force. Analysis was performed in triplicate to determine the R_a (average roughness), R_p (maximum peak height) and R_v (maximum valley depth).

2.2.3 Contact angle and surface energy

Contact angle measurements were performed by the sessile drop method with a CAM200 contact angle goniometer and SFECAM software (KSV Instruments, UK). Surface free energy (SFE) was calculated by use of the Fowkes method [33], which requires the contact angle measurement of three solvents of known polar and dispersive surface tension components; deionised water, diiodomethane (Sigma-Aldrich, UK) and ethylene glycol (Sigma-Aldrich, UK).

2.3 Antimicrobial analysis

2.3.1 Culture conditions and standardisation

Pseudomonas aeruginosa type strain NCTC 10332 and *S. aureus* NCTC 8178 were used throughout this study. All working stocks of *P. aeruginosa* NCTC 10332 and *S. aureus* NCTC 8178 were maintained at 4˚C on Luria Bertani agar (LB [Oxoid, Cambridge, UK]). *P. aeruginosa* NCTC 10332 and *S. aureus* NCTC 8178 were propagated in Luria Bertani broth (LB [Oxoid, Cambridge, UK]). Uncoated SS316, DLC coated SS316 and Ge-DLC coated SS316 were each positioned in wells of a 6-well plate. Prior to inoculation, substrates were disinfected by the addition of 2 ml 100% Ethanol (EtOH) to each well for 2 h. Following sterilisation, EtOH was aspirated, and the wells washed twice with deionised water (dH_2O) and 1 ml of LB broth added to each well. Overnight cultures of *P. aeruginosa* NCTC 10332 and *S. aureus* NCTC 8178 were washed by centrifugation at 7000 x *g* for 5 minutes, re-suspended in PBS and adjusted to an optical density (OD) at wavelength 570 nm of 0.3, which corresponds to $1x10^8$ CFU/ml. A working inoculum was prepared to $1x10^5$ CFU/ml. To each well, 1 ml of $1x10^5$ CFU/ml inoculum was added to give a final inoculum per well of $5x10^4$ CFU/ml. A sterile media control and sterile controls for uncoated and coated SS316 were included. Plates were

incubated for 24 h at 37°C, in air. Following incubation, spent growth media was aspirated and the resultant biofilms on substrates washed twice with 1x PBS and transferred to a clean 6-well plate for biomass analysis or fixing for SEM analysis.

2.3.2 Microbial biofilm assay

An adapted crystal violet (CV) biofilm assay for *P. aeruginosa* and *S. aureus* was performed [34]. To briefly summarise, filtered CV (Fisher, UK) was prepared to a 0.1% w/v solution in dH_2O. At the experimental end time point the coated discs were removed from the 6 well plates. Media supernatants were aspirated and the biofilm was washed twice with PBS to remove non-adherent cells. Two millilitres of 0.1% w/v CV was added to each well containing a substrate disc, including the media-only control discs. Samples were incubated at room temperature for 15 mins. Excess CV stain was removed by washing in dH_2O until subsequent washes did not visually remove any further excess staining. To quantify the bound CV, 2 ml 80% v/v ethanol was added and samples gently rocked to allow full desaturation of the biofilm, and the destained solution transferred to a 96 well flat bottom plate (n=6). This procedure was repeated for all substrates, controls, media control and an ethanol-only control. The optical density for the plate was read at OD_{595nm} using an Infinite F200 Pro plate reader (Tecan Group Ltd, Switzerland).

2.3.3 SEM analysis of biofilms on modified DLC coatings

Microbial biofilms of *P. aeruginosa* ATCC 10332 and *S. aureus* NCTC 8178 grown on SS316, DLC coated SS316 and Ge-DLC coated SS316 were prepared for SEM analysis as previously described [35]. Briefly, biofilms were fixed in a mixture of 2% paraformaldehyde, 2% glutaraldehyde, and 0.15% Alcian blue 8GX in 0.15 M sodium cacodylate buffer of pH 7.2 for 22 h. After primary fixation,

samples were washed three times in 0.15 M sodium cacodylate buffer for 15 minutes, then post fixed with 1% osmium tetroxide in 0.15 M sodium cacodylate buffer of pH 7.2 for 1 h. Samples were washed with dH2O three times and negative counter-stained by addition of 0.5% uranyl acetate for 1 h. Fixed and stained substrates were dehydrated using an ascending ethanol dehydration process (30%, 50%, 70%, 90%, absolute, dried absolute) twice for 15 minutes. Following dehydration, substrates were critically dried by addition of hexamethyldisilazane (HDMS) twice and stored in a desiccator overnight. Substrates were then coated with 5 nm of gold using an EMSscope SC500 sputter coater (EMS, UK). Examination of samples was performed in a Hitachi S-4100 scanning electron microscope under vacuum, operated at 10 kV.

2.4 Statistical analysis

Data were exported from the Infinite F200 Pro plate reader to Microsoft Excel (Microsoft, USA). Statistical analysis and graphing of data were performed in GraphPad Prism 6.0 (Graph Pad Software Inc, USA). The data were assessed for normality using column statistics analysis; statistical analysis was performed using the appropriate statistical test based on the assessment of the normality of the data. Statistical significance was achieved when $p < 0.05$.

3. Results and discussion

3.1 SEM and EDX evaluation of DLC and Ge-DLC

Analysis of the cross sectional SEM images of multilayer DLC and germanium-doped multilayer DLC coatings showed no visible delamination of the base layer from the Si wafer; this is in keeping with previous findings demonstrating the use of Si-DLC as a base layer in multilayer DLC to prevent film delamination from the surface [31]. Total coating thicknesses of 967 nm (DLC) and 1450 nm (Ge-DLC) (Figure 2A & 2B) were measured by SEM. It was noted that the top, or cap, layer of Ge-DLC was thicker than that of the DLC, indicating a faster film growth rate when TMGe is present in the

chamber. Composition of the top layer was determined by EDX analysis of the DLC and of the Ge-DLC on silicon witness pieces. A cross-sectional tilted SEM image of the Ge-DLC coating is shown in figure 2C, with two EDX spectra taken from the same sample shown in Figure 2D. These correspond to the sub-cap layer and the Ge-DLC cap layer. As expected, a significant quantity of germanium is incorporated into the cap layer, along with carbon and silicon. (It should be noted that there is also a significant fraction of hydrogen within all layers of the coatings deposited; however, this is not detectable by EDX [2]). Save for hydrogen, the interlayers comprise only carbon and silicon, showing that germanium is restricted to the cap layer as expected. Results of EDX quantitative analysis at increasing acceleration voltage (10, 15, 20 kV) are shown in Table 2. By EDX at 10 kV, Ge-DLC is composed of 28.9% germanium, 64.2% carbon, 5% silicon and 2% oxygen; DLC, in contrast, is composed of 87.8% carbon and 12.2% silicon. It is worthy of note that, at higher acceleration voltages, a small percentage of chromium and iron was detected; this is assumed to be due to sputtering and redeposition of constituents of the steel substrates during the early stages of the deposition process. Since all components of the chamber/pipe interior become coated with DLC during the deposition process, it is expected that these species are only present in the adhesion (first) coating layer; this is supported by EDX analysis, where the presence of chromium and iron is only detected at beam acceleration voltages >15kV, where the beam penetrates further into the sample.

Table 2. EDX compositional analysis of DLC and Ge-DLC

		Percentage (%)					
	Voltage	**Carbon**	**Silicon**	**Germanium**	**Chromium**	**Iron**	**Oxygen**
DLC	10 kV	87.8	12.2	-	-	-	-
	15 kV	83.9	15.6	-	0.2	0.2	-
	20 kV	84.4	15.2	-	0.2	0.2	-
Ge-DLC	10 kV	64.2	5	28.9	-	-	2
	15 kV	67	15.2	14.9	0.6	0.5	1.7
	20 kV	68.1	19	9.3	0.6	0.7	2.1

3.2 Physical characterisation

The surface roughness of uncoated SS316, DLC coated SS316 and Ge-DLC coated SS316 was measured by surface profilometer, with the measured R_a (average surface roughness) being 30.4 ± 12.4, 34.33 ± 10.2 and 21.47 ± 2.4 nm respectively. No significant difference in roughness between DLC (p = 0.6928) and Ge-DLC (p = 0.2879) was measured, though Ge-DLC showed lower average roughness than both uncoated SS316 and DLC. Wettability of the surfaces was determined by contact angle measurement with 3 solvents and SFE calculated; resultant data are summarised in Table 3 with *d*, *p* and *tot* subscripts denoting dispersive component, polar component and total dispersive plus polar SFE, respectively.

Table 3. Measurement of SFE components

Fowkes	Sfe_d (mN/m)	Sfe_p (mN/m)	Sfe_tot (mN/m)
SS316	30.25 ± 0.58	1.40 ± 0.17	31.63 ± 0.42
DLC	39.56 ± 1.17	4.03 ± 0.66	43.59 ± 1.69
Ge-DLC	24.93 ± 0.59	35.50 ± 1.56	60.42 ± 1.12

The contact angles and calculated surface free energy (SFE) for DLC were consistent with previously published values for a-C:H type DLC [36, 37]. A significant ($p < 0.0001$) increase in the polar component and concomitant decrease in the dispersive component of SFE was observed in the Ge-DLC coating; the overall surface energy is also approximately 40% greater than undoped modified DLC. This increase is solely linked to the incorporation of germanium in the cap layer; this, in turn, is explained by the relatively polar nature of the Ge-C bond, owing to a difference in electronegativity of 0.54 between carbon and germanium. Undoped modified DLC coating, in contrast, displays higher dispersive and lower polar SFE components, as is expected for a material dominated by carbon-carbon covalent bonding. The higher surface energy (and lower contact angle) of both DLC and Ge-DLC resulted in an increase in the wettability of the surface with respect to uncoated SS316. While protein adsorption and biofilm attachment are complex processes influenced by a host of factors including surface chemistry, physical topography and environmental conditions, other workers have shown that increased surface wettability may correlate with increased resistance to protein adsorption and biofouling. For example, with *S. epidermis* and *C. marina,* protein adsorption on hexa(ethylene glycol) terminated self-assembled monolayer (SAM) coatings is reported to increase with decreasing SFE [38]. Similarly, crosslinked PEG acrylate coatings have been reported to inhibit the attachment of BSA proteins, with higher wettability correlating with increased fouling resistance [39]. Such resistance corresponds to the high surface energy region of the Baier curve [40]. Additionally, it is also reported that increased presence of polar groups in alkylthiol-modified amorphous carbons also leads to decreased protein attachment and hence improved biofouling resistance [41]. This is particularly relevant given that Ge-DLC films prepared in this work exhibited significantly higher polar SFE component than DLC.

3.3 Antimicrobial analysis

Formation of biofilms by *P. aeruginosa* and *S. aureus* was observed on uncoated SS316, DLC coated SS316 and Ge-DLC coated SS316, indicating that total inhibition of biofilm formation by these coatings did not occur. Measured biomass showed no significant reduction in the biofilm formation of *S. aureus* by either modified DLC or by Ge-DLC, with the control biomass being measured at OD_{570nm} = 0.45 ± 0.19, DLC OD_{570nm} = 0.44 ± 0.14 and Ge-DLC OD_{570nm} = 0.32 ± 0.16 (Figure 3). However, significant reduction in *P. aeruginosa* biofilm formation was observed on both DLC (OD_{570nm} = 0.16 ±0.02, 54.4% reduction) and Ge-DLC (OD_{570nm} = 0.137 ± 0.01, 62.6% reduction), when compared to the uncoated control (OD_{570nm} = 0.37 ± 0.19). The small difference in biomass reduction (11.2%) between DLC and Ge-DLC was not statistically significant ($p > 0.05$); however, it was decided to investigate the biofilm formed using SEM to determine any structural effect on the biofilm and cells. In keeping with the results showing no significant reduction in biofilm formation of *S. aureus*, biofilms were confluent with no cellular disruption noted (Figure 4D-F). In contrast, *P. aeruginosa* biofilms were sparse on all substrates; there was no evidence of disruption of the cells on DLC (Figures 4A & 4B). However, *P. aeruginosa* cells on Ge-DLC (Figure 4C) showed visible disruption to the outer cell wall and leakage of cellular components. *P. aeruginosa* cell disruption was only observed with those biofilms grown on Ge-DLC surfaces, indicating that incorporation of germanium into the carbon matrix may be responsible for this effect; with the caveat that further studies are needed in order to more fully elucidate the point.

The primary mechanism of action of most metals and metal nanoparticles is the disruption of the cell wall and of other cellular components [42]. There is, however, still uncertainty in the exact mechanisms. For example, opinion is divided on the mechanism of action of silver, with its antimicrobial capacity being attributed to depletion of ATP levels [43] or the blockage of microbial DNA replication [44]. It is as of yet unclear whether the mechanism of action of metal doped DLC

films are the same as those of the elemental metals or if they are altered. Tributyltin (TBT) was, until relatively recently, widely employed as a biocide and marine antifouling agent, though has latterly been largely withdrawn due to environmental concerns. TBT itself is a cytotoxic compound, whose mechanism of action is apoptosis via elevation of calcium concentration and generation of reactive oxygen species in mitochondria [45]. It may be speculated that the cap layer coating, being chemically somewhat similar to an organogermanium compound, is operating by a similar mechanism with regard to Gram-negative bacteria. There is some evidence, however, that *P. aeruginosa* has developed resistance to TBTs [46, 47]; indeed, there are TBT-resistant bacteria from several Gram-negative and Gram-positive species, including *Staphylococcus* spp. and *Pseudomonas* spp. [45].

Other workers have reported that organogermanium compounds, particularly lactones containing organogermanium, exhibit a highly selective antibacterial effect against Gram-negative bacilli [48]. This agrees well with our results; these suggest that Ge-DLC may exhibit an antibacterial effect with respect to *P. aeruginosa*. However, the mechanism by which Ge-DLC appears to precipitate the disruption of the cell requires further research, and further studies with regard to Ge doping level are required to gain a more comprehensive understanding of this effect

4. Conclusion

Modified multilayer DLC was deposited on SS316 discs by pulsed-DC hollow cathode plasma enhanced chemical vapour deposition (PECVD). In the case of Ge-DLC, germanium was incorporated in the cap layer only. The surface energy of multilayer DLC and Ge-DLC exhibited a significantly increased total surface energy and resultant wettability when compared to modified DLC; additionally, the polar component of surface energy for Ge-DLC is significantly larger.
No significant reduction in biofilm formation was observed with *S. aureus* biofilms, this likely due to differences between the cell wall thickness and composition of Gram-positive (*S. aureus*) and Gram-

negative (*P. aeruginosa*) bacteria. *P. aeruginosa* biofilm formation was significantly reduced with both DLC and Ge-DLC, compared to uncoated SS316. SEM analysis of *P. aeruginosa* cells on Ge-DLC showed disruption of the cell wall and possible indication of the inhibition of cell separation; this effect was not apparent with modified DLC. Further investigations of this apparent antimicrobial effect are planned; as well as of the role, and concentration dependence, of germanium doping in Ge-DLC, in terms of possible antimicrobial activity.

Acknowledgments

The authors would like to thank Harry Staines for useful statistical discussion and his interest in this work. We also thank Dr Liz Porteous for laboratory assistance. We are grateful for the financial support provided by QNIS, STFC [Grant number ST/M00726X/1], SUPA, The Royal Society, and The University of the West of Scotland.

References

[1] H.C. Flemming, Biofouling in water systems--cases, causes and countermeasures, Appl Microbiol Biotechnol, 59 (2002) 629-640.
[2] R. Birney, Design, Deposition and Characterisation of Protective Modied Multilayered Diamond-Like Carbon Thin Films, PhD Thesis, University of the West of Scotland, 2012.
[3] D. Enning, J. Garrelfs, Corrosion of iron by sulfate-reducing bacteria: new views of an old problem, Appl Environ Microbiol, 80 (2014) 1226-1236.
[4] M.P. Schultz, J.A. Bendick, E.R. Holm, W.M. Hertel, Economic impact of biofouling on a naval surface ship, Biofouling, 27 (2011) 87-98.
[5] W.R. Mac Kenzie, N.J. Hoxie, M.E. Proctor, M.S. Gradus, K.A. Blair, D.E. Peterson, J.J. Kazmierczak, D.G. Addiss, K.R. Fox, J.B. Rose, et al., A massive outbreak in Milwaukee of cryptosporidium infection transmitted through the public water supply, N Engl J Med, 331 (1994) 161-167.
[6] M. Widerstrom, C. Schonning, M. Lilja, M. Lebbad, T. Ljung, G. Allestam, M. Ferm, B. Bjorkholm, A. Hansen, J. Hiltula, J. Langmark, M. Lofdahl, M. Omberg, C. Reuterwall, E. Samuelsson, K. Widgren, A. Wallensten, J. Lindh, Large outbreak of Cryptosporidium hominis infection transmitted through the public water supply, Sweden, Emerg Infect Dis, 20 (2014) 581-589.
[7] J.M. Jefferies, T. Cooper, T. Yam, S.C. Clarke, Pseudomonas aeruginosa outbreaks in the neonatal intensive care unit--a systematic review of risk factors and environmental sources, J Med Microbiol, 61 (2012) 1052-1061.
[8] D. de Beer, P. Stoodley, F. Roe, Z. Lewandowski, Effects of biofilm structures on oxygen distribution and mass transport, Biotechnol Bioeng, 43 (1994) 1131-1138.
[9] J.R. Lawrence, D.R. Korber, B.D. Hoyle, J.W. Costerton, D.E. Caldwell, Optical sectioning of microbial biofilms, J Bacteriol, 173 (1991) 6558-6567.
[10] K. Vickerya, A. Devaa, A. Jacombsa, J. Allana, P. Valentea, I.B. Gosbellb, Presence of biofilm containing viable multiresistant organisms despite terminal cleaning on clinical surfaces in an intensive care unit, Journal of Hospital Infection, 80 (2013) 52-55.
[11] M. Corcoran, D. Morris, N. De Lappe, J. O'Connor, P. Lalor, P. Dockery, M. Cormican, Commonly used disinfectants fail to eradicate Salmonella enterica biofilms from food contact surface materials, Appl Environ Microbiol, 80 (2014) 1507-1514.
[12] J.P. Folsom, J.F. Frank, Chlorine resistance of Listeria monocytogenes biofilms and relationship to subtype, cell density, and planktonic cell chlorine resistance, J Food Prot, 69 (2006) 1292-1296.
[13] T. Casserly, K. Boinapally, M. Oppus, D. Upadhyaya, B. Boardman, A. Tudhope, Investigation of DLC-Si film deposited inside a 304SS pipe using a novel hollow cathode plasma immersion ion processing method, Proceedings of the Society of Vacuum Coaters Annual Technical Conference, DOI (2007).
[14] D. Pech, N. Schupp, P. Steyer, T. Hack, Y. Gachon, C. Heau, A.S. Loir, J.C. Sanchez-Lopez, Duplex SiCN/DLC coating as a solution to improve fretting-Corrosion resistance of steel, Wear, 266 (2009) 832-838.
[15] R. Sharma, P.K. Barhai, N. Kumari Corrosion resistant behaviour of DLC films, Thin Solid Films, 516 (2008) 5397-5403.
[16] M.M. R.D. Mansano, A.P. Mousinho, Z. Zambom, and L.G. Neto, Protective carbon layer for chemical corrosion of stainless steel, Diamond and Related Materials, 12 (2003) 749-752.
[17] C. Liu, Q. Zhao, Y. Liu, S. Wang, E.W. Abel, Reduction of bacterial adhesion on modified DLC coatings, Colloids Surf B Biointerfaces, 61 (2008) 182-187.
[18] Q. Zhao, Y. Liu, C. Wang, S. Wang, Evaluation of bacterial adhesion on Si-doped diamond-like carbon films, Applied Surface Science, 253 (2007) 7254-7259.

[19] Y.H. Chan, C.F. Huang, K.L. Ou, P.W. Peng, Mechanical properties and antibacterial activity of copper doped diamond-like carbon films, Surf Coat Tech, 206 (2011) 1037-1040.
[20] N. Harrasser, S. Jussen, I.J. Banke, R. Kmeth, R. von Eisenhart-Rothe, B. Stritzker, H. Gollwitzer, R. Burgkart, Antibacterial efficacy of titanium-containing alloy with silver-nanoparticles enriched diamond-like carbon coatings, AMB Express, 5 (2015) 77.
[21] A. Adamcakova-Dodd, L.V. Stebounova, J.S. Kim, S.U. Vorrink, A.P. Ault, P.T. O'Shaughnessy, V.H. Grassian, P.S. Thorne, Toxicity assessment of zinc oxide nanoparticles using sub-acute and sub-chronic murine inhalation models, Part Fibre Toxicol, 11 (2014) 15.
[22] A.P. Ingle, N. Duran, M. Rai, Bioactivity, mechanism of action, and cytotoxicity of copper-based nanoparticles: a review, Appl Microbiol Biotechnol, 98 (2014) 1001-1009.
[23] A.M. Studer, L.K. Limbach, L. Van Duc, F. Krumeich, E.K. Athanassiou, L.C. Gerber, H. Moch, W.J. Stark, Nanoparticle cytotoxicity depends on intracellular solubility: comparison of stabilized copper metal and degradable copper oxide nanoparticles, Toxicol Lett, 197 (2010) 169-174.
[24] X. Yang, A.P. Gondikas, S.M. Marinakos, M. Auffan, J. Liu, H. Hsu-Kim, J.N. Meyer, Mechanism of silver nanoparticle toxicity is dependent on dissolved silver and surface coating in Caenorhabditis elegans, Environ Sci Technol, 46 (2012) 1119-1127.
[25] S. Buchegger, C. Vogel, R. Herrmann, B. Stritzker, A. Wixforth, C. Westerhausen, Antibacterial metal ion release from diamond-like carbon modified surfaces for novel multifunctional implant materials, Journal of Materials Research, 31 (2016) 2571-2577.
[26] S.M. Moskowitz, J.M. Foster, J. Emerson, J.L. Burns, Clinically feasible biofilm susceptibility assay for isolates of Pseudomonas aeruginosa from patients with cystic fibrosis, J Clin Microbiol, 42 (2004) 1915-1922.
[27] T. Bjarnsholt, K. Kirketerp-Moller, S. Kristiansen, R. Phipps, A.K. Nielsen, P.O. Jensen, N. Hoiby, M. Givskov, Silver against Pseudomonas aeruginosa biofilms, APMIS, 115 (2007) 921-928.
[28] A.L.Q. Khalid, B.A. AlJohny, M. Wainwright, Antibacterial effects of pure metals on clinically important bacteria growing in planktonic cultures and biofilms, African Journal of Microbiology Research, 8 (2014) 1080-1088.
[29] D. Lusk, T. Casserly, M. Gupta, K. Boinapally, Y. Cao, R. Ramamurti, P. Desai, A High Density Hollow Cathode Plasma PECVD Technique for Depositing Films on the Internal Surfaces of Cylindrical Substrates, Plasma Process Polym, 6 (2009) S429-S432.
[30] D. Lusk, M. Gore, W. Boardman, T. Casserly, K. Boinapally, M. Oppus, D. Upadhyaya, A. Tudhope, M. Gupta, Y. Cao, S. Lapp, Thick DLC films deposited by PECVD on the internal surface of cylindrical substrates, Diamond and Related Materials, 17 (2008) 1613-1621.
[31] R. Birney, F. Placido, J. Kavanagh, Characterisation and Comparison of Diamond-Like Carbon Thin Films Deposited by RF-PECVD and Pulsed-DC Hollow Cathode PECVD, Society of Vacuum Coaters, 54th Annual Technical Conference Proceedings (2011).
[32] B.J. Jones, L. Anguilano, J.J. Ojeda, Argon plasma treatment techniques on steel and effects on diamond-like carbon structure and delamination, Diamond and Related Materials, 20 (2011) 1030-1035.
[33] D.Y. Kwok, A.W. Neumann, Contact angle measurement and contact angle interpretation, Advances in Colloid and Interface Science, 81 (1999) 167-249.
[34] G.A. O'Toole, Microtiter dish biofilm formation assay, J Vis Exp, 47 (2011).
[35] S.L. Erlandsen, C.J. Kristich, G.M. Dunny, C.L. Wells, High-resolution visualization of the microbial glycocalyx with low-voltage scanning electron microscopy: dependence on cationic dyes, J Histochem Cytochem, 52 (2004) 1427-1435.
[36] M. Grischke, A. Hieke, F. Morgenweck, H. Dimigen, Variation of the wettability of DLC-coatings by network modification using silicon and oxygen, Diamond and Related Materials, 7 (1998) 454-458.
[37] J. Robertson, Diamond-like amorphous carbon, Mat Sci Eng R, 37 (2002) 129-281.

[38] L.K. Ista, H. Fan, O. Baca, G.P. Lopez, Attachment of bacteria to model solid surfaces: oligo(ethylene glycol) surfaces inhibit bacterial attachment, FEMS Microbiol Lett, 142 (1996) 59-63.
[39] H. Ju, B.D. McCloskey, A.C. Sagle, V.A. Kusuma, B.D. Freeman, Preparation and characterization of crosslinked poly(ethylene glycol) diacrylate hydrogels as fouling-resistant membrane coating materials, Journal of Membrane Science, 330 (2009) 180-188.
[40] C.M. Magin, S.P. Cooper, A.B. Brennan, Non-toxic antifouling strategies, Materials Today, 13 (2010) 36-44.
[41] F. Zen, M.D. Angione, J.A. Behan, R.J. Cullen, T. Duff, J.M. Vasconcelos, E.M. Scanlan, P.E. Colavita, Modulation of Protein Fouling and Interfacial Properties at Carbon Surfaces via Immobilization of Glycans Using Aryldiazonium Chemistry, Sci Rep, 6 (2016) 24840.
[42] M. Yasuyuki, K. Kunihiro, S. Kurissery, N. Kanavillil, Y. Sato, Y. Kikuchi, Antibacterial properties of nine pure metals: a laboratory study using *Staphylococcus aureus* and *Escherichia coli*, Biofouling, 26 (2010) 851-858.
[43] C.N. Lok, C.M. Ho, R. Chen, Q.Y. He, W.Y. Yu, H. Sun, P.K. Tam, J.F. Chiu, C.M. Che, Proteomic analysis of the mode of antibacterial action of silver nanoparticles, Journal of proteome research, 5 (2006) 916-924.
[44] Q.L. Feng, J. Wu, G.Q. Chen, F.Z. Cui, T.N. Kim, J.O. Kim, A mechanistic study of the antibacterial effect of silver ions on *Escherichia coli* and *Staphylococcus aureus*, Journal of biomedical materials research, 52 (2000) 662-668.
[45] A. Cruz, A.M. Anselmo, S. Suzuki, S. Mendo, Tributyltin (TBT): A Review on Microbial Resistance and Degradation, Critical Reviews in Environmental Science and Technology, 45 (2015) 970-1006.
[46] J.J. Cooney, Organotin Compounds and Aquatic Bacteria - a Review, Helgolander Meeresuntersuchungen, 49 (1995) 663-677.
[47] K. Fukushima, S.K. Dubey, S. Suzuki, YgiW homologous gene from *Pseudomonas aeruginosa* 25W is responsible for tributyltin resistance, J Gen Appl Microbiol, 58 (2012) 283-289.
[48] Z. Amtul, C. Follmer, S. Mahboob, R. Atta Ur, M. Mazhar, K.M. Khan, R.A. Siddiqui, S. Muhammad, S.A. Kazmi, M.I. Choudhary, Germa-gamma-lactones as novel inhibitors of bacterial urease activity, Biochemical and biophysical research communications, 356 (2007) 457-463.

List of Captions

Figure 1. Sample arrangement in chamber and schematic of deposition system
An aluminium stage was fabricated to conform to the internal diameter of a 4" pipe. Left image shows substrates (SS316 with Si witness piece) loaded on the aluminium stage and aluminium foil lining of the pipe chamber. Gas entry head anode is visible in background. Right image shows simplified schematic of deposition apparatus.

Figure 2. Characterisation of DLC and Ge-DLC on silicon
SEM cross sectional analysis of total thickness (A) Five layer modified DLC on silicon wafer (B) Five layer Ge-DLC on silicon wafer (C) Tilted cross section of Ge-DLC on silicon wafer, indicated sampling points for EDX marked (D) EDX spectra of Ge-DLC cap layer (yellow) and the interlayer composed of carbon and silicon (no fill black line).

Figure. 3. Effect of DLC and Ge-DLC on 24 h biofilm formation of *P. aeruginosa* and *S. aureus*.
Comparison of biofilm formation on uncoated SS316, DLC coated SS316 and germanium doped DLC coated SS316 with *P. aeruginosa* and *S. aureus*. Data are mean ± Standard deviation. n = 3, *** $p < 0.001$, ** $p < 0.01$

Figure 4. SEM analysis of microbial biofilms on substrates
(A) *P. aeruginosa* on SS316 (B) *P. aeruginosa* on DLC (C) *P. aeruginosa* on Ge-DLC (D) *S. aureus* on SS316 (E) *S. aureus* on DLC (F) *S. aureus* on Ge-DLC. Scale bar = 5 µm

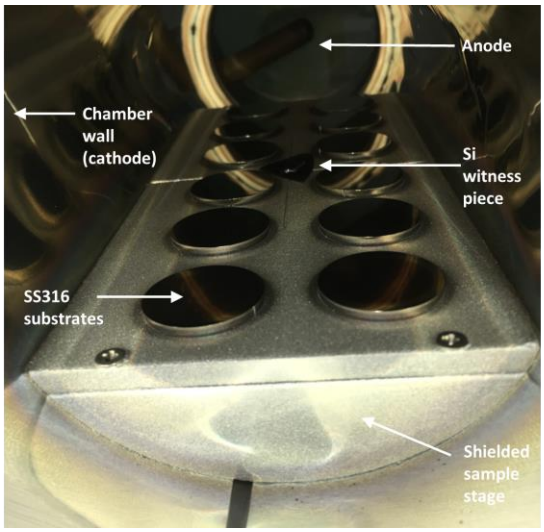
Anode
Chamber wall (cathode)
Si witness piece
SS316 substrates
Shielded sample stage

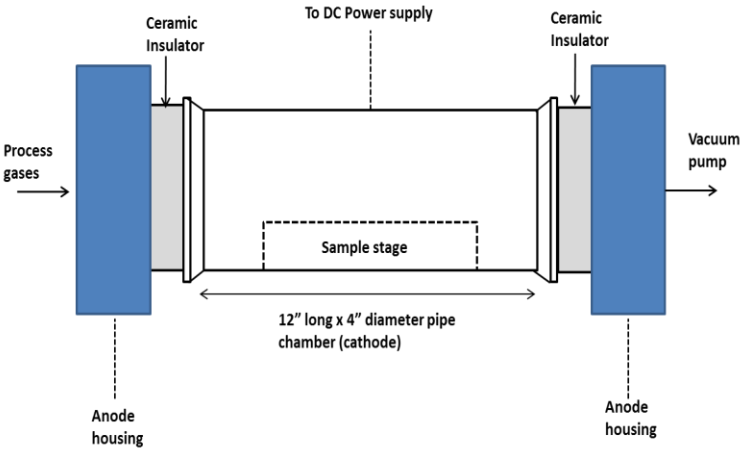
Ceramic Insulator
To DC Power supply
Ceramic Insulator
Process gases
Vacuum pump
Sample stage
12" long x 4" diameter pipe chamber (cathode)
Anode housing
Anode housing

1.

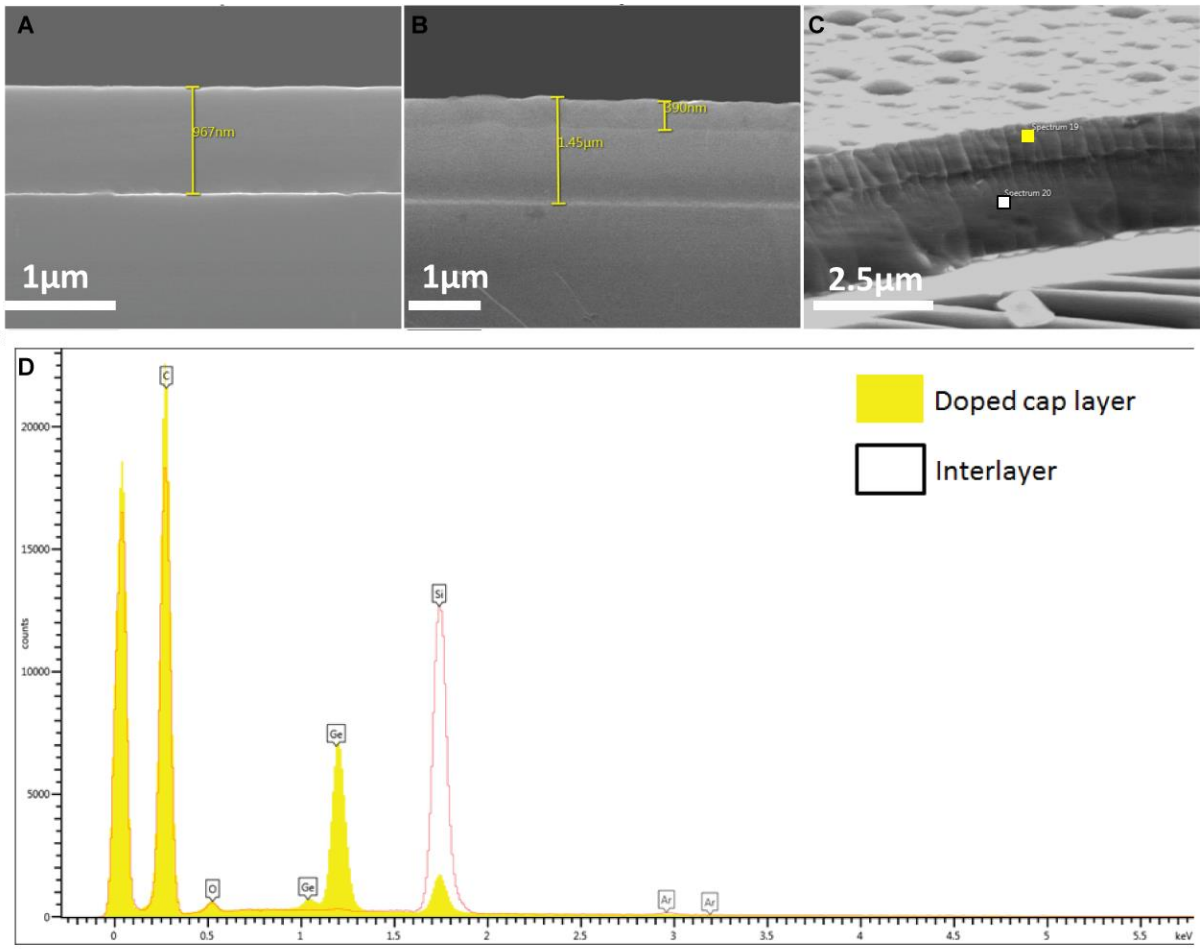
A
967nm
1µm
B
390nm
1.45µm
1µm
C
Spectrum 19
Spectrum 20
2.5µm
D
Doped cap layer
Interlayer
counts
keV

2.

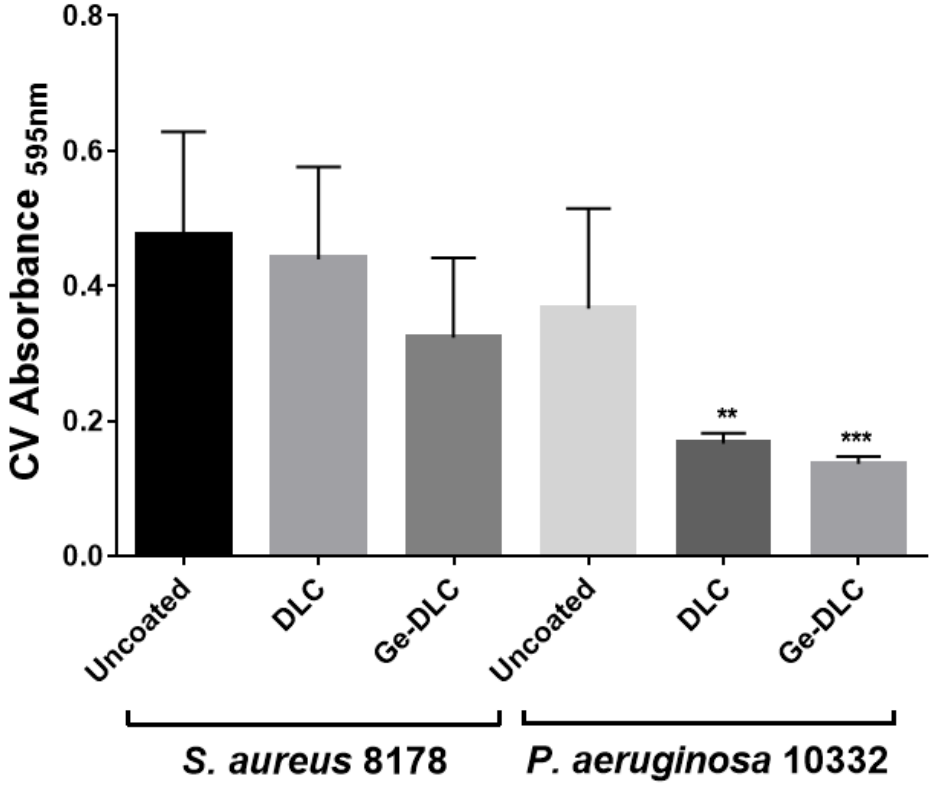
CV Absorbance 595nm
0.8
0.6
0.4
0.2
0.0
**
***
Uncoated
DLC
Ge-DLC
Uncoated
DLC
Ge-DLC
S. aureus 8178
P. aeruginosa 10332

3.

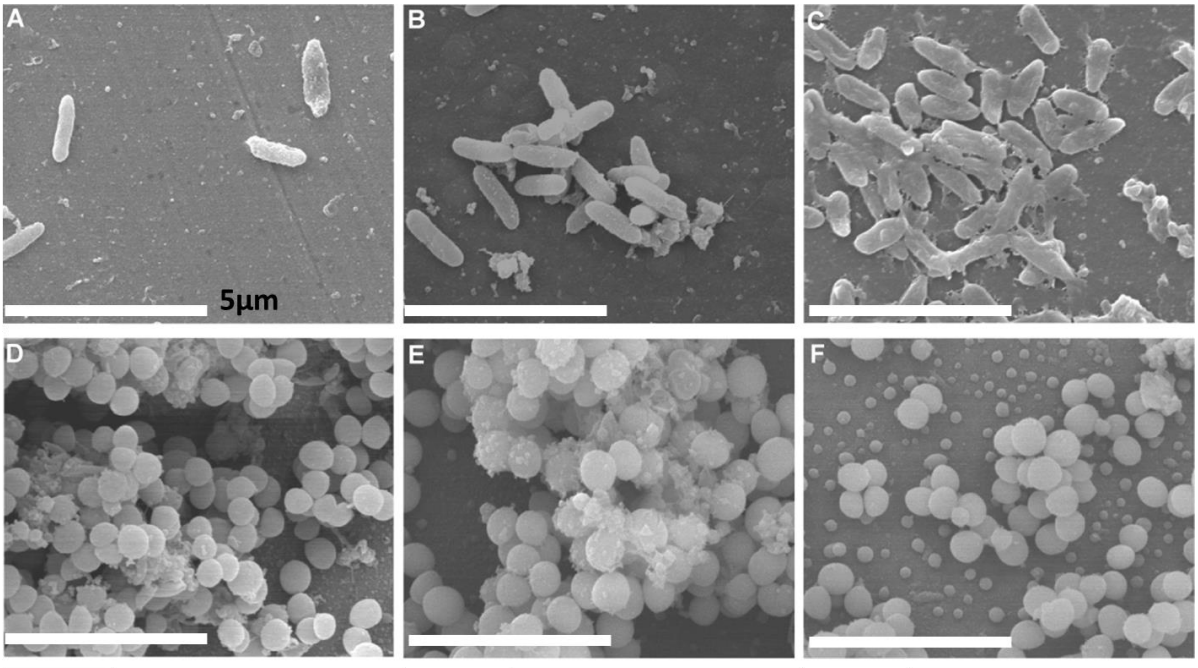
A
B
C
5µm
D
E
F

4.